ESC European Society of Cardiology

European Heart Journal - Digital Health (2023) **4**, 473–487
https://doi.org/10.1093/ehjdh/ztad050

ORIGINAL ARTICLE

Electrocardiographic temporo-spatial assessment of depolarization and repolarization changes after epicardial arrhythmogenic substrate ablation in Brugada syndrome

Emanuela T. Locati [1,†], Peter M. Van Dam [2,3,†], Giuseppe Ciconte [1], Francesca Heilbron [4], Machteld Boonstra [2], Gabriele Vicedomini [1], Emanuele Micaglio [1], Žarko Ćalović[1], Luigi Anastasia [1,5], Vincenzo Santinelli [1], and Carlo Pappone [1,5,*]

[1]Arrhythmology-Electrophysiology Department, IRCCS Policlinico San Donato, Piazza Malan 2, 20097 San Donato Milanese, Milan, Italy; [2]Cardiology Department, Utrecht University Medical Center, Heidelberglaan 100, 3584 CX, Utrecht, Netherlands; [3]Center for Digital Medicine and Robotics, Jagiellonian University Medical College, Kopernika 7e, 31-034 Kraków, Poland; [4]Milano Bicocca University, Istituto Auxologico, Via Thomas Mann 8, 20162 Milan, Italy; and [5]Vita-Salute San Raffaele University, Via Olgettina 58, 20132 Milan, Italy

Received 20 April 2023; revised 16 August 2023; accepted 25 August 2023; online publish-ahead-of-print 6 September 2023

Aims In Brugada syndrome (BrS), with spontaneous or ajmaline-induced coved ST elevation, epicardial electro-anatomic potential duration maps (epi-PDMs) were detected on a right ventricle (RV) outflow tract (RVOT), an arrhythmogenic substrate area (AS area), abolished by epicardial-radiofrequency ablation (EPI-AS-RFA). Novel CineECG, projecting 12-lead electrocardiogram (ECG) waveforms on a 3D heart model, previously localized depolarization forces in RV/RVOT in BrS patients. We evaluate 12-lead ECG and CineECG depolarization/repolarization changes in spontaneous type-1 BrS patients before/after EPI-AS-RFA, compared with normal controls.

Methods and results In 30 high-risk BrS patients (93% males, age 37 + 9 years), 12-lead ECGs and epi-PDMs were obtained at baseline, early after EPI-AS-RFA, and late follow-up (FU) (2.7–16.1 months). CineECG estimates temporo-spatial localization during depolarization (Early-QRS and Terminal-QRS) and repolarization (ST-Tpeak, Tpeak-Tend). Differences within BrS patients (baseline vs. early after EPI-AS-RFA vs. late FU) were analysed by Wilcoxon signed-rank test, while differences between BrS patients and 60 age–sex-matched normal controls were analysed by the Mann–Whitney test. In BrS patients, baseline QRS and QTc durations were longer and normalized after EPI-AS-ATC (151 ± 15 vs. 102 ± 13 ms, $P < 0.001$; 454 ± 40 vs. 421 ± 27 ms, $P < 0.000$). Baseline QRS amplitude was lower and increased at late FU (0.63 ± 0.26 vs. 0.84 ± 13 ms, $P < 0.000$), while Terminal-QRS amplitude decreased (0.24 ± 0.07 vs. 0.08 ± 0.03 ms, $P < 0.000$). At baseline, CineECG depolarization/repolarization wavefront prevalently localized in RV/RVOT (Terminal-QRS, 57%; ST-Tpeak, 100%; and Tpeak-Tend, 61%), congruent with the AS area on epi-PDM. Early after EPI-AS-RFA, RV/RVOT localization during depolarization disappeared, as Terminal-QRS prevalently localized in the left ventricle (LV, 76%), while repolarization still localized on RV/RVOT [ST-Tpeak (44%) and Tpeak-Tend (98%)]. At late FU, depolarization/repolarization forces prevalently localized in the LV (Terminal-QRS, 94%; ST-Tpeak, 63%; Tpeak-Tend, 86%), like normal controls.

Conclusion CineECG and 12-lead ECG showed a complex temporo-spatial perturbation of both depolarization and repolarization in BrS patients, prevalently localized in RV/RVOT, progressively normalizing after epicardial ablation.

* Corresponding author. Tel: +390252774260/4306, Email: carlo.pappone@grupposandonato.it
†The first two authors contributed equally to the study.

Graphical Abstract

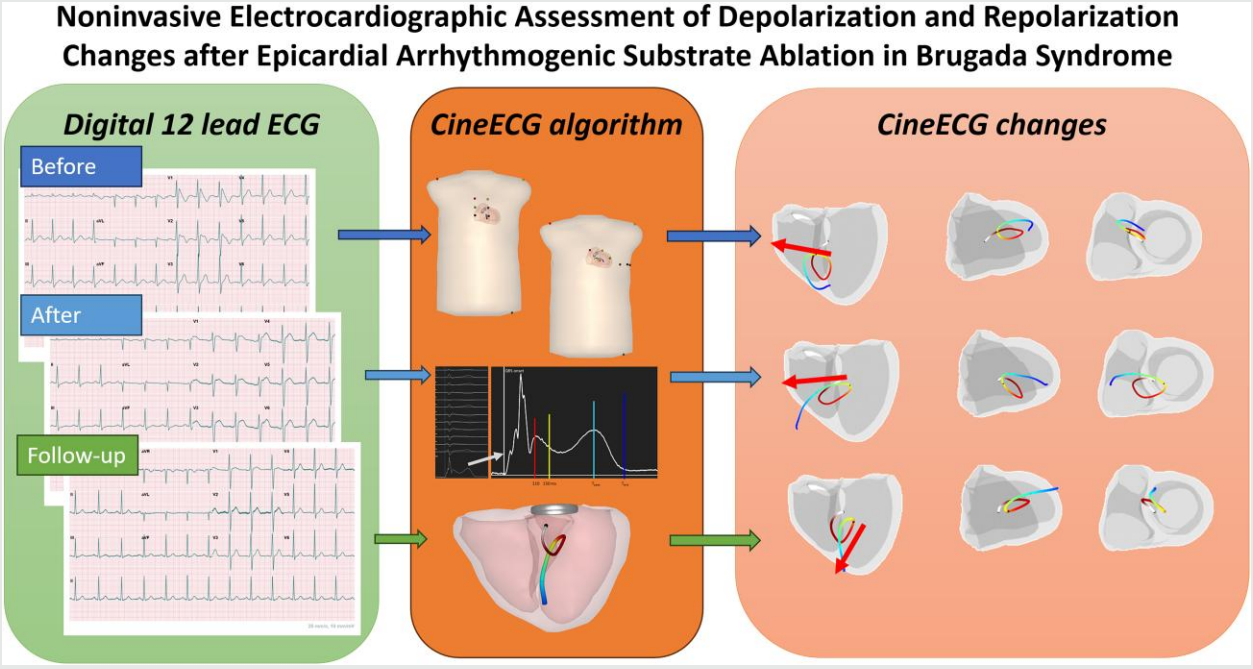

Keywords Brugada syndrome • Electrocardiogram • Cardiac ablation • Sudden death • Depolarization • Repolarization

Introduction

Brugada syndrome (BrS) is an inherited disorder with high risk of sudden cardiac death (SCD) from ventricular tachycardia/fibrillation (VT/VF) in young otherwise healthy patients.[1–3] The 12-lead electrocardiogram (ECG) shows a typical coved ST-segment elevation in anterior precordial leads (type-1 BrS pattern), either spontaneous or induced by sodium-channel blockers (ajmaline or flecainide). *SCN5A* gene mutations, occurring in ~25–30% of BrS cases, are considered causative and have been associated with a worse prognosis, while mutations described in other genes have still unknown implications on pathogenesis and prognosis.[4,5]

Experimental and clinical studies demonstrated that in BrS, VT/VF originate from the epicardial right ventricle outflow tract (RVOT). Either body-surface mapping[6,7] or epicardial electro-anatomical mapping[8,9] demonstrated an area of conduction delay and fragmented potentials in RVOT, defined as arrhythmogenic substrate (AS). Previous studies showed that the AS area, measured by epicardial potential duration maps (epi-PDMs), is maximized by ajmaline infusion, and can be removed by epicardial-radiofrequency application (EPI-AS-RFA), also abolishing type-1 BrS pattern and VT/VF inducibility.[10–12] EPI-AS-ATC was demonstrated safe and effective in high-risk Brugada patients.[10–13] The AS area was associated with signal-averaged late-potentials, possible expression of abnormal epicardial electrical activity.[14] While initially BrS was considered as a purely electric disease, recently RV mechanical abnormalities were observed on 3D echocardiography[15] and in nuclear magnetic resonance imaging.[16]

Two main hypotheses have been proposed as BrS pathophysiological mechanism as follows: the 'depolarization hypothesis', relying on RV conduction slowing and involvement of mild structural abnormalities, and the 'repolarization hypothesis', relying on transmural dispersion of repolarization between RVOT endocardium and epicardium.[17,18] Even if AS characteristics rather support delayed depolarization as pathogenic mechanism, both hypotheses are still under debate.

To elucidate the origin of BrS pattern, we recently develop the novel non-invasive CineECG method, derived from 12-lead ECGs by inverse ECG method, localizing the temporo-spatial cardiac waveforms in a 3D-heart model.[19–22] Our previous studies with CineECG showed that in BrS patients, the terminal ventricular depolarization forces were localized to RVOT, consistent with the AS area detected by epi-PDMs, both in spontaneous and ajmaline-induced BrS patients.[21] Vice versa, RVOT localization of late depolarization was never found in normal subjects, in right bundle branch block (RBBB), or in ajmaline-negative patients.[21,23] In our initial CineECG study, we did not examine ventricular repolarization, and so far, only few studies focused on repolarization in BrS patients, with inconclusive results.[9,24]

Aims of this study were as follows: (i) to identify the temporo-spatial localization of both depolarization and repolarization wavefront by 12-lead ECG and CineECG in 30 BrS patients with spontaneous type-1 pattern, in comparison with 60 age- and sex-matched normal controls and (ii) to evaluate both 12-lead ECG and CineECG changes occurring early and late following epicardial substrate ablation within the same BrS patients.

Methods

Study population

Brugada patients

We included 30 high-risk BrS patients with spontaneous type-1 Brugada pattern on baseline 12-lead ECG, Italy, prospectively enrolled in 'San Donato Brugada Syndrome Registry Study' (NCT02641431 and

NCT03106701), who underwent epicardial arrhythmogenic substrate ablation (epi-EPI-AS-RFA) at 'IRCCS Policlinico San Donato', Milan. Details on the study protocol have been already published.[11,12] All BrS patients were inducible for sustained VT or VF at programmed ventricular stimulation (PVS) and had received an implantable cardiac defibrillator (ICD) before undergoing EPI-AS-RFA.[11,12] The local Institutional Review Board approved the study protocols, and all patients provided written consent after being fully informed about the potential risks and benefits before undergoing this investigational procedure requiring general anaesthesia. Definition used to identify type-1 BrS pattern was derived from latest Brugada Consensus Document.[1] None of these patients had been included in our previous CineECG study cohort.[21]

Normal controls

The control group included 60 age–sex-matched normal subjects, with negative personal and familial history of cardiac disease, without cardiac medication, whose 12-lead digital ECGs were extracted from certified Physionet PTB-Diagnostic ECG-Database https://www.physionet.org/content/ptb-xl/1.0.1/.[25]

Electro-anatomical mapping

All BrS patients at baseline underwent epicardial electro-anatomical mapping using a 3D-mapping system (CARTO3, Biosense Webster, CA, USA), as previously described.[12] Epicardial maps were obtained before and after ajmaline infusion (up to 1 mg/kg in 5 min), at baseline and early after EPI-AS-RFA. Epicardial potential duration maps (epi-PDMs) were computed from epicardial electrograms (EGMs) durations. Colour-coded PDMs showed the regions displaying shortest durations in red (<110 ms) and longest in purple (>160 ms). The AS was defined as the area (in cm^2) with EGMs above 110 ms duration, computed both before and after ajmaline.[12]

Arrhythmogenic substrate ablation

The AS, characterized by prolonged fragmented ventricular potentials, was eliminated by using low-energy radiofrequency application (EPI-AS-RFA), as already described.[10–12] Arrhythmogenic substrate abolition was confirmed by epi-PDM obtained early after EPI-AS-RFA, before and after ajmaline infusion, together with BrS pattern elimination and VT/VF non-inducibility.

Follow-up control visits

All BrS patients underwent prospective follow-up (FU) control visits, at 3-6-12–18 months after EPI-AS-RFA, and at each FU, digital 12-lead ECGs were obtained before and after ajmaline infusion.[12] The latest FU ECG available for each patient was utilized for analysis (mean FU time 7.0 ± 4.6 months, range 3–18 months). During the follow-up, after ablation, all patients remained asymptomatic.

CineECG method

CineECG, obtained from 12-lead ECGs by inverse method, correlated the cardiac activation pathway to the cardiac anatomy, by projecting the temporo-spatial localization of CineECG wavefront to a 3D-heart model representing the ventricles (*Figure 1A*).[19–22] The technology underlying CineECG method is described in detail in Supplementary material online, *Appendix-A* (CineECG Methodology). In summary, to compute the CineECG, the electrode positions on the torso model were used to construct the vectorcardiogram (VCG), as ECG amplitude weighted sum of lead vectors, as previously described.[22] As the 12-lead ECGs of BrS patients and controls may have different electrode placement configurations, CineECG method automatically corrected for electrode position.[21,22] CineECG method was shown to be relative insensitive to limited changes in electrode placement, including the parasternal precordial lead placements.[22] While the VCG represented the direction of electrical forces from a point inside the heart, the CineECG was constructed by the average position of electrical forces at fixed time steps relative to the heart model, using as starting point the left septal position, closest to the centre of ventricular mass (*Figure 1A*). According to previous studies,[21,22] the CineECG temporal resolution was 1 ms, with a spatial resolution of 0.7 mm/ms.

In this study, differently with our previous CineECG studies, we analysed both depolarization and repolarization by projecting the wavefront localizations at each time interval during the entire cardiac cycle on the 3D-heart mode.[22]Thus, the CineECG represents the instant summation of multiple depolarization and repolarization wavefront, providing the temporo-spatial localization of cardiac activation and recovery, anchored at mid-QRS as temporal reference and at the central mass of the 3D-heart model.[22] The moving 3D representation of the average temporo-spatial isochrone localization for a normal control was also available as CineECG Movie (see Supplementary material online, *Web-Movie S1*).

Twelve-lead electrocardiogram parameters

From 6–8 averaged beats with similar QRS morphology, QRS onset was automatically set when the root-mean-square (RMS) amplitude steadily increased for at least 10 ms and QRS offset was automatically set as the time when the RMS reached the lowest amplitude after the QRS peak (*Figure 1B*). To evaluate the late activation/early repolarization phase, we defined the interval ranging from 110 to 150 ms after QRS onset as Terminal-QRS and measured its amplitude (mV) (*Figure 1B*). We selected the time reference of 110 ms as the standard upper limit for normal QRS duration while 150 ms as the average duration for RBBB and BrS pattern.[26] The repolarization time (ST-Tend) was defined as the interval from 150 ms to T-wave end (Tend). The T-wave end (Tend) was defined at the intersection of the tangent to the T-wave downslope with the isoelectric line, while T-wave peak (Tpeak) was set at the maximum RMS.[27] The ST-Tpeak interval ranged from 150 ms to Tpeak, while Tpeak-Tend interval from Tpeak to Tend (*Figure 1B*). The maximum QRS and Tpeak amplitude were also computed from the RMS.

CineECG definitions

The CineECG showed the progression of activation and recovery wavefront towards three distinct cardiac areas, septum, left ventricle (LV), and right ventricle (RV) including RVOT, visualized by the three standard cardiac views as follows: four chambers, right and left anterior oblique [right anterior oblique (RAO) and left anterior oblique (LAO), *Figure 1C*]. To quantify the CineECG trajectory, two CineECG parameters were defined as follows[21]:

- CineECG location was computed as the percentage of CineECG-time spent into the three cardiac areas [septum, LV, and RV/RVOT, during specific time intervals (e.g. 100% LV meaning that CineECG was totally located in LV during a given time interval)]. CineECG location was determined during depolarization for entire QRS and Terminal-QRS, and during repolarization for ST-Tend, ST-Tpeak, and Tpeak-Tend intervals. From previous CineECG studies, in normal subjects, the initial location of depolarization occurred in the septum, then moving to LV during depolarization, remaining close to the septum.[21]
- CineECG direction represented the congruence with the orthogonal cardiac axes (posterior–anterior, right–left, and apex–base). The CineECG directions were quantified by a number between −1 and +1 (+1 indicating total congruence and −1 indicating an opposite direction relative to a given axis) (*Figure 1C*). The CineECG direction was computed for all time intervals during both repolarization and depolarization.

CineECG classes from previous studies,[21,23] we defined four diagnostic CineECG classes, based on the following criteria as follows:

(1) 'Normal': QRS duration < 110 ms, Terminal-QRS location in RV/RVOT < 50%, Terminal-QRS direction towards LV.
(2) 'Brugada': QRS duration ≥ 110 ms, Terminal-QRS location in RV/RVOT > 50%, Terminal-QRS direction towards RV/RVOT, average Terminal-QRS amplitude > 0.1 mV.
(3) 'RBBB': QRS duration ≥ 110 ms, Terminal-QRS location in RV/RVOT > 50%, Terminal-QRS direction towards RV/RVOT.
(4) 'Undetermined': not matching any of the above criteria.

Statistical analysis

Statistical analysis was performed by SPSS (IBM SPSS Statistics for Windows, Version 26.0.0.1. Armonk, NY: IBM Corp.). Data were given as

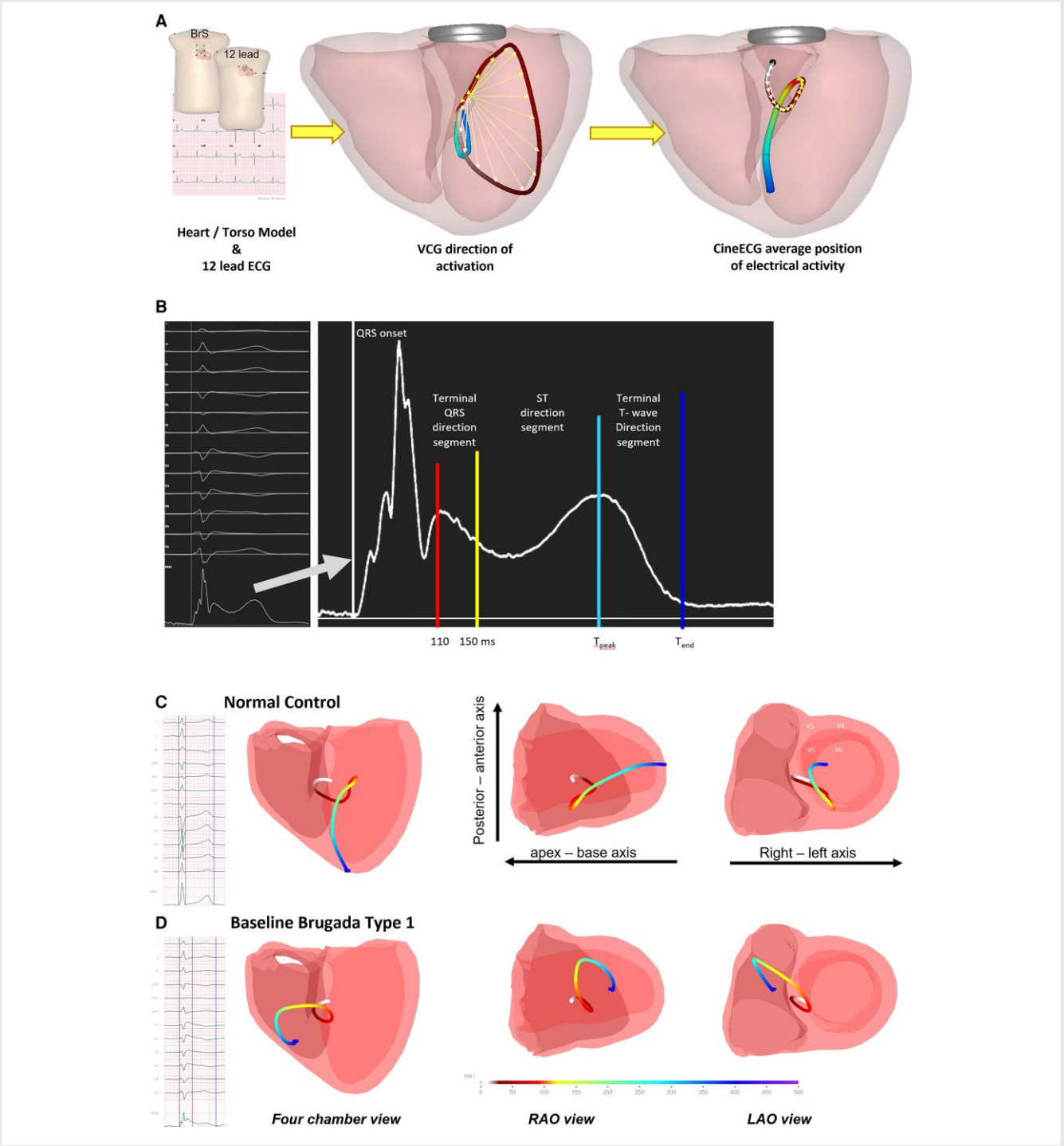

Figure 1 CineECG activation pathway construction and examples. Panel *A* shows the construction of the CineECG from the 12-lead ECG in combination with a heart/torso model of a normal 58-year-old male with either the standard 12-lead electrode configuration or the parasternal Brugada syndrome (BrS) lead system. Combining the ECG and heart/torso model enables the computation of the vectorcardiogram (VCG), indicated by a coloured line from white (QRS onset) to blue (T-wave end). The VCG direction over time is shown by several vectors. The VCG direction is used to construct the activation pathway of the QRS, indicated by similarly coloured arrows with fixed 3D length. Panel *B* shows the QRS fiducial points from 12-lead ECG. QRS onset is indicated by the white vertical line. The interval 110–150 ms after QRS onset was defined as terminal QRS (between red and yellow lines); the interval between 150 ms after QRS onset and the T-wave peak (light blue line) was defined as ST-Tpeak, and the interval between T-wave peak and T-wave end (blue line) was defined as Tpeak-Tend. In panel *C*, ventricles are projected in standard cardiac views as follows: four chambers, right anterior oblique (RAO) and left anterior oblique (LAO), the right ventricle (RV) is in dark red, and left ventricle (LV) in light red. The coloured arrow depicts the CineECG to the ventricle from QRS onset to T-wave end (right: colour bar from white to blue). Initial trans-septal vector is in white, the T-wave end in blue. On the left, the original 12-lead ECG tracings. Upper lower panel: normal subject, panel *D*, Brugada patient at baseline. BrS, Brugada syndrome; VCG, vectorcardiogram; RAO, right anterior oblique; LAO, left anterior oblique; RV, right ventricle; LV, left ventricle.

Table 1 Demographic and clinical characteristics of patients with Brugada syndrome ($n = 30$)

Male sex (*n*, %)	28 (93%)
Mean age [years, mean ± SD, (range)]	37 ± 9 (18–53)
Body mass index [mean ± SD, (range)]	21.2 ± 2.3 (16.2–27.8)
Spontaneous type-1 BrS pattern on 12-lead ECG (*n*, %)	30 (100%)
Previous VF inducibility/ICD implantation (*n*, %)	30 (100%)
BrS Shanghai score	5.3 ± 1.2 (3.5–9.0)
History of typical BrS symptoms (*n*, %)[a]	14 (47%)
Familial history of BrS and/or unexplained sudden death (*n*, %)[b]	22 (73%)
AS area at baseline [cm^2, mean ± SD, (range)]	5.7 ± 7.6 (0–26.3)
AS area during ajmaline infusion [cm^2, mean ± SD, (range)]	19.3 ± 4.2 (10.4–27.7)
Mean follow-up interval [months, mean ± SD, (range)]	6.4 ± 4.2 (2.7–16.1)
Genetic testing available (*n*, %)	30 (100%)
Patients with mutation in BrS associated genes[c] (*n*, %)	8 (26.7%)

[a]Two patients had previous aborted cardiac arrest, seven patients had previous history of syncope of likely arrhythmic origin), five had history of sustained palpitations with recording of non-sustained ventricular tachycardia.
[b]Family history of BrS was present in 12 patients, family history of sudden death in 10 patients.
[c]Five patients carry pathogenic variants in SCN5A gene, two had variants of uncertain significance in SCN10A and one in CACNA1C.

mean ± standard deviation (SD), and ranges (minimum–maximum), for variables with normal distribution, and as median and ranges for non-parametric variables. Wilcoxon related-samples signed-rank Test for paired samples was used for non-parametric variables to analyse repeated ECG measurements within BrS patients at baseline vs. early after EPI-AS-RFA vs. at late follow-up. Mann–Whitney non-parametric tests for independent samples were used to analyse differences between normal controls and BrS patients at baseline, early after EPI-AS-RFA, and at late follow-up. A 0.05 *P* significance level was used for both pairwise and unpaired comparisons. The complete statistical analysis was provided as Supplementary material online, *Supplement Web Material* (Statistical Analysis Results).

Results

Clinical characteristics of Brugada syndrome patients

All 30 BrS patients (93% males, age 37 ± 9 years) had spontaneous type-1 BrS pattern on 12-lead ECG (*Tables 1* and *2*). No patient had overt cardiac abnormalities by echocardiography and nuclear magnetic resonance tests. All patients were inducible for sustained VT or VF during PVS, and all had ICD implanted before EPI-AS-RFA. The mean Shanghai Score[28] of the patients was 5.3 ± 1.2 (range 3.5–9). Most patients (73%) had familial history of BrS and/or unexplained SCD, and 40% of them had previous history of typical BrS-related symptoms [cardiac arrest or syncope of highly likely arrhythmic origin or sustained palpitations with recording of non-sustained VT (NSVT)], while the remaining had atypical BrS-related symptoms, including syncope of uncertain origin, dizziness, and chest pain, with recording of NSVT. Genetic testing was available in all the cases, five patients (19%) carrying pathogenic variants in *SCN5A* gene, while two patients carrying variants of uncertain significance in *SCN10A* gene and one patient in *CACNA1C* gene, while the remaining did not show mutations in known BrS-related genes.

Epicardial potential duration maps of Brugada syndrome patients at baseline and early after arrhythmogenic substrate ablation

At baseline, the average AS area on RV/RVOT at epi-DBM was 5.7 + 7.6 cm^2 (range 0–26.3 cm^2). After ajmaline infusion, the AS average area was 21 cm^2 (range 16.2–26.5 cm^2) (*Table 1*, *Figure 3*). The individual tracings of substrate area, 12-lead ECG, and CineECG are provided in Supplementary material online, *Appendix-B* (Individual Patients' Material). After EPI-AS-RFA, in all patients, both type-1 and AS disappeared, and EGM duration at epi-PDM uniformly fell below 110 ms.

Twelve-lead electrocardiogram and CineECG characteristics

The results of 12-lead ECG and CineECG analyses in the 30 BrS patients at baseline, early after EPI-AS-RFA, and at late follow-up and in the 60 age- and sex-matched controls are provided in *Tables 2–4*.

Twelve-lead electrocardiogram and CineECG characteristics of age- and sex-matched normal controls

The mean QRS, ST-Tpeak, Tpeak-Tend, and QTc durations and the maximum QRS, terminal QRS, and Tpeak amplitudes computed from the RMS of the 12-lead ECGs in the 60 age–sex-matched normal controls are provided in *Table 2*. As to CineECG spatial location, the initially depolarization localized in the septum, then moving to the LV, both for depolarization (QRS and terminal QRS) and repolarization (ST-Tpeak and Tpeak-Tend) (*Table 3*, *Figures 2* and *3*, Supplementary material online, *Web-Movie S1*). In normal controls, CineECG activity localized prevalently in LV, during both depolarization and repolarization, while it never localized in RV/RVOT (*Table 3*). CineECG directions both during Terminal-QRS and during repolarization were prevalent to the apex (*Table 4*, *Figures 4* and *5*). All controls were classified as 'Normal' by CineECG criteria (*Table 5*).

Twelve-lead electrocardiogram and CineECG characteristics of Brugada syndrome patients at baseline

At baseline, all BrS patients presented a typical type-1 BrS pattern at 12-lead ECG. The mean QRS, ST-Tpeak, Tpeak-Tend, and QTc durations and the maximum QRS, terminal-QRS, and Tpeak amplitudes computed from the RMS of the 12-lead ECGs in the 30 BrS patients are provided in *Table 2*. The individual 12-lead ECG tracings are

Table 2 Standard ECG parameters for Brugada patients ($n = 30$) (at baseline, early after arrhythmogenic substrate radiofrequency ablation and at late follow-up) and normal age- and sex-matched controls ($n = 60$)

ECG Parameters mean ± SD (min–max)	QRS duration (ms)	ST-Tpeak interval (ms)	Tpeak-Tend interval (ms)	QT interval (ms)	RR interval (ms)	QTc (ms)	Max QRS amplitude (ms)	Terminal-QRS amplitude (mV)	Max T peak amplitude (mV)
BrS patients at baseline ($n = 30$)	151 ± 15 (124–175)	140 ± 34 (21–201)	122 ± 25 (91–201)	413 ± 32 (354–484)	845 ± 181 (592–1050)	454 ± 40 (388–562)	0,63 ± 0,26 (0,37–1,46)	0.20 ± 0.07 (0.11–0.49)	0.24 ± 0.06 (0.09–0.37)
BrS patients early after epi-AS-RFA ($n = 30$)	110 ± 17 (77–154)	110 ± 39 (37–188)	153 ± 27 (98–213)	413 ± 40 (324–513)	815 ± 113/ 809 (641–1140)	460 ± 48 (380–574)	0,61 ± 0,22 (0,34–1,24)	0.20 ± 0.09 (0.09–0.47)	0.31 ± 0.11 (0.13–0.52)
BrS patients at late follow-up ($n = 30$)	102 ± 13 (83–137)	126 ± 23 (74–166)	108 ± 16 (84–149)	384 ± 26 (322–445)	844 ± 159 (571–1200)	421 ± 27 (378–478)	0,84 ± 0,33 (0,47–2,05)	0.08 ± 0.03 (0.03–0.12)	0.26 ± 0.11 (0.12–0.53)
Normal controls ($n = 60$)	88 ± 8 (71–109)	138 ± 27 (75–220)	100 ± 12 (79–145)	388 ± 28 (326–460)	899 ± 156 (565–1331)	412 ± 23 (360–460)	1,05 ± 0,28 (0,58–2,23)	0.07 ± 0.03 (0.04–0.15)	0.35 ± 0.09 (0.18–0.66)
Adjusted significance by Bonferroni correction for multiple pairwise comparisons within Brugada patients									
BrS patients at baseline vs. early after epi-AS-RFA	0.001	0.001	0.001	NS	NS	NS	NS	NS	0.000
BrS patients at baseline vs. late follow-up	0.001	NS	NS	0.002	NS	0.029	0.000	0.000	NS
BrS patients at early after AS-RFA vs. late follow-up	NS	NS	0.000	0.001	NS	0.001	0.000	0.000	0.02
Significance for multiple pairwise comparisons by Mann–Whitney *U* test between BrS patients and normal controls									
Normal controls vs. BrS patients at baseline	0.000	NS	0.000	0.002	0.045	0.000	0.000	0.000	0.000
Normal controls vs. BrS patients early after AS-RFA	0.000	0.000	0.000	0.002	0.008	0.000	0.000	0.000	0.03
Normal controls vs. BrS patients at late follow-up	0.000	0.038	0.019	NS	NS	NS	0.018	NS	0.000

All standard ECG parameters were measured on the root-mean-square (RMS) of the 12-lead ECG (see *Methods* for details). QTc = QT interval corrected by the Bazett formula, and Terminal-QRS is the interval from 110–150 ms after QRS onset; ST-Tpeak indicates the interval from 150 ms after QRS onset to T-wave peak, and Tpeak-Tend indicates the interval from T-wave peak to T-wave end (see *Methods* for details).
NS, not significant (>0.05); AS-RFA, arrhythmogenic substrate radiofrequency ablation.

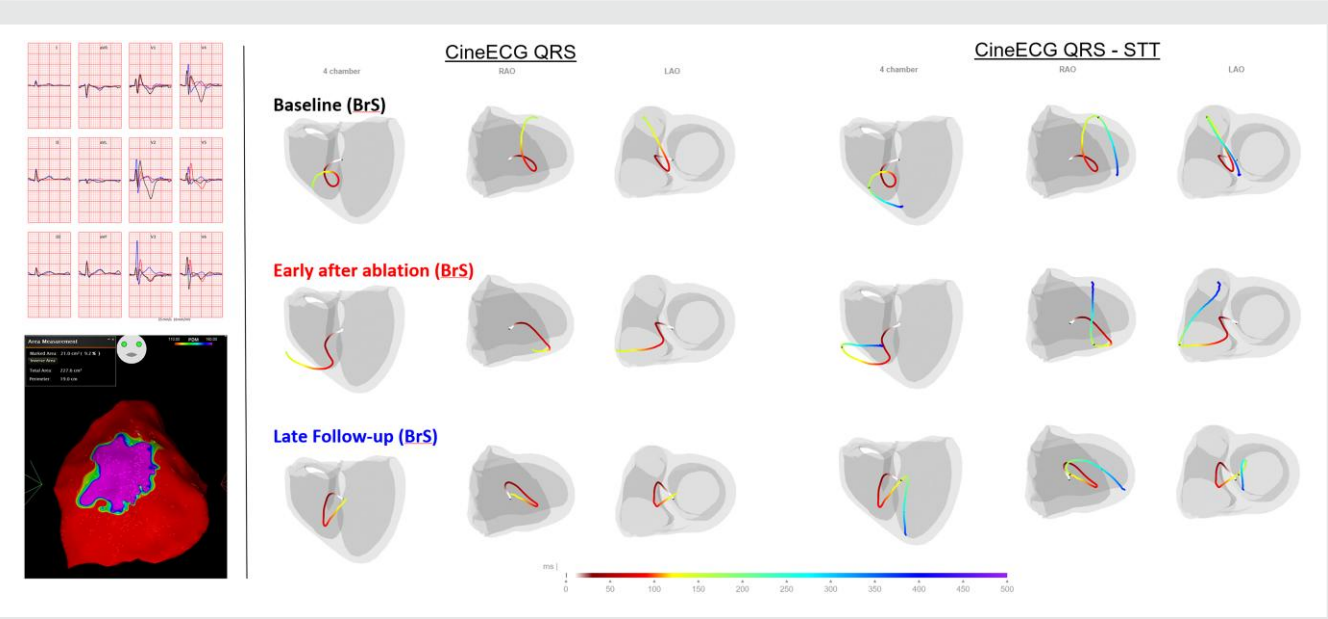

Figure 2 12-Lead ECG tracings, CineECGs, and epicardial potential duration map (epi-PDM) in a Brugada patient. Left-upper panel: overlapping 12-lead tracings obtained before (black), early after arrhythmogenic substrate (AS) radiofrequency ablation (EPI-AS-RFA, red), and at late follow-up (blue). Left-lower panel: colour-coded epi-PDM at baseline during ajmaline infusion, displaying regions with shortest (red) and longest (purple) potential durations, utilizing a 110–160 ms cut-off, determining the AS area, localized on right ventricular outflow tract (RVOT) and right ventricle (RV) epicardium. Middle panel: CineECG activation pathway before (above) and at follow-up (below) during QRS. Right panel: CineECG activation pathway before (above) and at follow-up (below) during STT (patient no. 6, male, age 41 years, substrate area: 21.0 cm^2, QRS duration 172 ms at baseline, 153 ms at early after EPI-AS-RFA, 137 ms at late follow-up) (see Supplementary material online, *Supplement B Web Materials* for Individual Brugada Patients). epi-PDM, epicardial potential duration map; EPI-AS-RFA, arrhythmogenic substrate (AS) radiofrequency ablation; RVOT, right ventricular outflow tract; RV, right ventricle.

provided in Supplementary material online, *Appendix-B* Individual Patients' Material. Of note, QRS and QTc durations were significantly longer in BrS patients at baseline than in normal controls, while maximum QRS, Terminal-QRS, and Tpeak amplitudes were significantly larger in BrS patients at baseline than in controls (*Table 2*).

As to CineECG depolarization parameters, the Terminal-QRS location was prevalent in RV/RVOT (median 57%) (*Table 3*), and terminal-QRS direction was mainly moving towards RVOT/RV, away from septum and LV, congruent with the posterior–anterior axis (*Figures 2–5*, *Table 4*). Of note, the Terminal-QRS location in RVOT corresponded to the AS location identified by epi-PDMs (*Figures 2–5*, Supplementary material online, *Web-Movie S2*, Supplementary material online, *Appendix-B* Individual Patients' Material).

During repolarization, in BrS patients at baseline, CineECG location and direction were prevalent in RVOT/RV, both during ST-Tpeak (median 100%) and Tpeak-Tend (median 61%) (*Tables 3* and *4*, *Figures 2–5*). As to CineECG classification, all BrS patients at baseline were classified 'Brugada' (*Table 5*).

Twelve-lead electrocardiogram and CineECG characteristics of Brugada syndrome patients early after epicardial arrhythmogenic substrate ablation

Early after EPI-AS-RFA, the type-1 pattern disappeared in 12-lead ECG in all BrS patients, while modest non-Brugada-like ST elevation appeared in most patients, and QRS interval significantly shortened with respect to baseline, while QTc was unchanged (*Table 2*, *Figure 2*, Supplementary material online, *Appendix-B* Individual Patients' Material).

Most CineECG depolarization parameters early after EPI-AS-RFA were already significantly different from baseline, as the terminal-QRS-CineECG location was no longer prevalent in RV/RVOT (median terminal-QRS RVOT location 0%), but it moved towards LV (median 76%) (*Table 3*, *Figures 2–5*, Supplementary material online, *Web-Movie S3*). In contrast, early after EPI-AS-RFA during repolarization, ST-Tpeak and Tpeak-Tend locations remained prevalent in RV/RVOT (respectively median 44% and 98%) (*Table 3*), while the ST-Tpeak and Tpeak-Tend directions started to normalize (*Table 4*, *Figures 4* and *5*). As to CineECG classification, early after EPI-AS-RFA, 67% of patients were now classified as 'Normal', while 10% were still classified as 'Brugada', 20% as 'Undetermined', and 3% as 'RBBB' (*Table 5*).

Twelve-lead electrocardiogram and CineECG characteristics of Brugada syndrome patients at late follow-up after epicardial arrhythmogenic substrate ablation

At late FU (mean FU time 7.0 ± 4.6 months, range 3–18 months), in all BrS patients, the 12-lead ECG type-1 pattern was no longer present, and QRS duration and morphology became generally normal (see Supplementary material online, *Appendix-B* Individual Patients' Material). Of interest, maximum QRS amplitude significantly increased at late FU compared to baseline, and terminal-QRS amplitude was significantly reduced, while no significant changes in mean T_{peak} amplitude were observed (*Table 2*).

All CineECG depolarization and repolarization parameters normalized, with CineECG locations becoming prevalent in LV, both for Terminal-QRS (median 76%), ST-Tpeak (median 63%), and Tpeak-Tend (median 86%) (*Table 3*, *Figures 2* and *3*), and CineECG directions mainly shifting towards septum/apex LV (congruent with right–left and

Table 3 CineECG location for Brugada patients ($n = 30$) (at baseline, early after epi-AS-RFA, and at late follow-up) and normal age- and sex-matched controls ($n = 60$)

CineECG parameters median (min–max)	QRS-CineECG location (%)			ST-Tend-CineECG location (%)			Terminal-QRS-CineECG location (%)			ST-Tpeak-CineECG location (%)			Tpeak-Tend-CineECG location (%)		
	Septum	LV	RV	Septum	LV	RV	Septum	LV	RV	Septum	LV	RV	Septum	LV	RV
BrS patients at baseline ($n = 30$)	45	21	26	1	12	78	34	0	57	0	0	100	0	12	61
	(23–70)	(0–67)	(0 –72)	(0–39)	(0–83)	(17–100)	(0–88)	(0–95)	(0–100)	(0–48)	(0–73)	0–100)	(0–58)	(0–100)	(0–100)
BrS patients early after epi-AS-RFA ($n = 30$)	38	29	16	21	14	69	8	76	0	38	7	44	0	0	98
	(11–78)	(0–89)	(0–84)	(0–53)	(0–100)	(0–100)	(0–95)	(0–100)	(0–100)	(0–92)	(0–100)	(0–100)	(0–56)	(0 –100)	(0–100)
BrS patients at late follow-up ($n = 30$)	46	47	0	11	74	0	1	94	0	10	63	0	0	86	0
	(1–77)	(1–99)	(0–79)	(0 78)	(0–100)	(0–100)	(0–100)	(0–100)	(0–100)	(0 95)	(0–100)	(0–100)	(0–88)	(0–100)	(0–100)
Normal controls ($n = 60$)	45	51	0	9	90	0	0	100	0	12	86	0	3	93	0
	(1–73)	(5–99)	(0–29)	(0–77)	(6–100)	(0–68)	(0–100)	(0–100)	(0–100)	(0–96)	(0–100)	(0–85)	(0–90)	(0–100)	(0–77)
Adjusted significance by Bonferroni correction for multiple pairwise comparisons within Brugada patients															
BrS patients at baseline vs. early after AS-RFA	NS	NS	NS	0.011	NS	NS	NS	0.002	0.004	0.000	NS	0.017	NS	NS	NS
BrS patients at baseline vs. late Follow-up	NS	0.00	< 0.01	NS	0.000	0.000	NS	0.000	0.000	0.035	0.000	0.000	NS	NS	0.029
BrS patients at early after epi-AS-RFA vs. late follow-up	NS	0.006	NS	NS	0.011	0.007	NS	NS	NS	NS	0.006	NS	NS	0.000	0.000
Significance for multiple pairwise comparisons by Mann–Whitney *U* test between BrS patients and normal controls															
Normal controls vs. BrS patients at baseline	NS	0.000	0.000	0.012	0.000	0.000	0.002	0.000	0.000	0.003	0.000	0.000	0.035	0.000	0.000
Normal controls vs. BrS patients early after AS-RFA	NS	0.000	0.001	NS	0.000	0.000	NS	0.002	0.009	0.039	0.000	0.000	NS	0.000	0.000
Normal controls vs. BrS patients at late follow-up	NS	NS	NS	NS	NS	NS	NS	NS	NS	NS	NS	NS	NS	NS	NS

CineECG location indicates the per cent time spent in each cardiac site (septum/left ventricle (LV)/right ventricle (RV); Terminal-QRS indicates the interval 110–150 ms after QRS onset; ST-Tend indicates the interval from 150 ms after QRS onset to the T-wave end; ST-Tpeak indicates the interval from 150 ms after QRS onset to T-wave peak, Tpeak-Tend indicates the interval from T-wave peak to T-wave end (see *Methods* for details).
AS-RFA, arrhythmogenic substrate radiofrequency ablation.

Table 4 CineECG directions for Brugada patients ($n = 30$) (at baseline, early after arrhythmogenic substrate radiofrequency ablation, and at late follow-up) and normal controls ($n = 60$)

Variables median min/max	Terminal-QRS-CineECG direction axis congruence (−1/+1)			STpeak-CineECG direction axis congruence (−1/+1)			Tpeak-Tend-CineECG Direction axis congruence (−1/+1)		
	x (RVOT/RV)	*y* (LV)	*z* (base)	*x* (RVOT/RV)	*y* (LV)	*z* (base)	*x* (RVOT/RV)	*y* (LV)	*z* (base)
BrS patients at baseline ($n = 30$)	0.43	−0.80	−0.16	−0.22	0.02	−0.81	−0.65	0.48	−0.52
	0.03/0.89	−0.98/−0.10	−0.73/0.53	−0.26/0.59	−0.82/0.98	−1.0/0.08	−0.84/−0.19	−0.24/0.92	−0.90/−0.06
BrS patients early after AS-RFA ($n = 30$)	0.42	−0.74	−0.32	0.27	−0.71	−0.54	−0.20	−0.29	−0.85
	−0.16/0.8	−0.92/−0.37	−0.85/0.50	−0.33/0.87	−0.94/0.48	−0.97/0.06	−0.59–0.76	−0.65/0.62	−0.99/−0.03
BrS patients at late follow-up ($n = 30$)	0.10	−0.69	−0.33	−0.17	−0.04	−0.90	−0.19	0.40	−0.76
	−0.81/0.84	−0.97/0.89	−0.98/0.66	−0.71/0.47	−0.85/0.53	−0.99/−0.51	−0.76—−0.67	−0.52/0.86	−0.97/−0.20
Normal controls ($n = 60$)	0.10	−0.50	−0.65	0.12	−0.17	−0.92	−0.02	0.39	−0.89
	−0.56/0.84	−0.97/0.45	−0.97/−0.27	−0.26/0.58	−0.86/0.51	−0.99/−0.41	−0.46–0.26	−0.63/0.68	−0.99/−0.70
Adjusted significance by Bonferroni correction for multiple pairwise comparisons within Brugada patients									
BrS patients at baseline vs. early after AS-RFA	NS	NS	NS	0.000	0.000	0.004	0.000	0.000	0.000
BrS patients at baseline vs. late follow-up	0.001	NS	NS	NS	NS	NS	0.009	NS	0.000
BrS patients at early after AS-RFA vs. late follow-up	0.006	NS	NS	0.000	0.000	0.000	NS	0.000	NS
Pairwise comparisons significance using the Mann–Whitney *U* test between BrS patients and normal controls									
Normal controls vs. BrS patients at baseline	0.000	0.002	0.000	0.000	NS	0.008	0.000	NS	NS
Normal controls vs. BrS patients early after AS-RFA	0.000	0.006	0.000	0.020	0.000	0.000	0.002	0.000	NS
Normal controls vs. BrS patients at late follow-up	NS	NS	0.002	0.000	NS	NS	0.000	NS	NS

CineECG direction indicates the orientation of activation according to *x*–*y*–*z*-axes where +1 indicates the maximum congruence, while −1 the opposite direction; Terminal-QRS indicates the interval 110–150 ms after QRS onset; STT indicates the interval from 150 ms after QRS onset to the T-wave end; STpeak indicates the interval from 150 ms after QRS onset to T-wave peak, and Tpeak-Tend indicates the interval from T-wave peak to T-wave end (see *Methods* for details).
AS-RFA, arrhythmogenic substrate radiofrequency ablation.

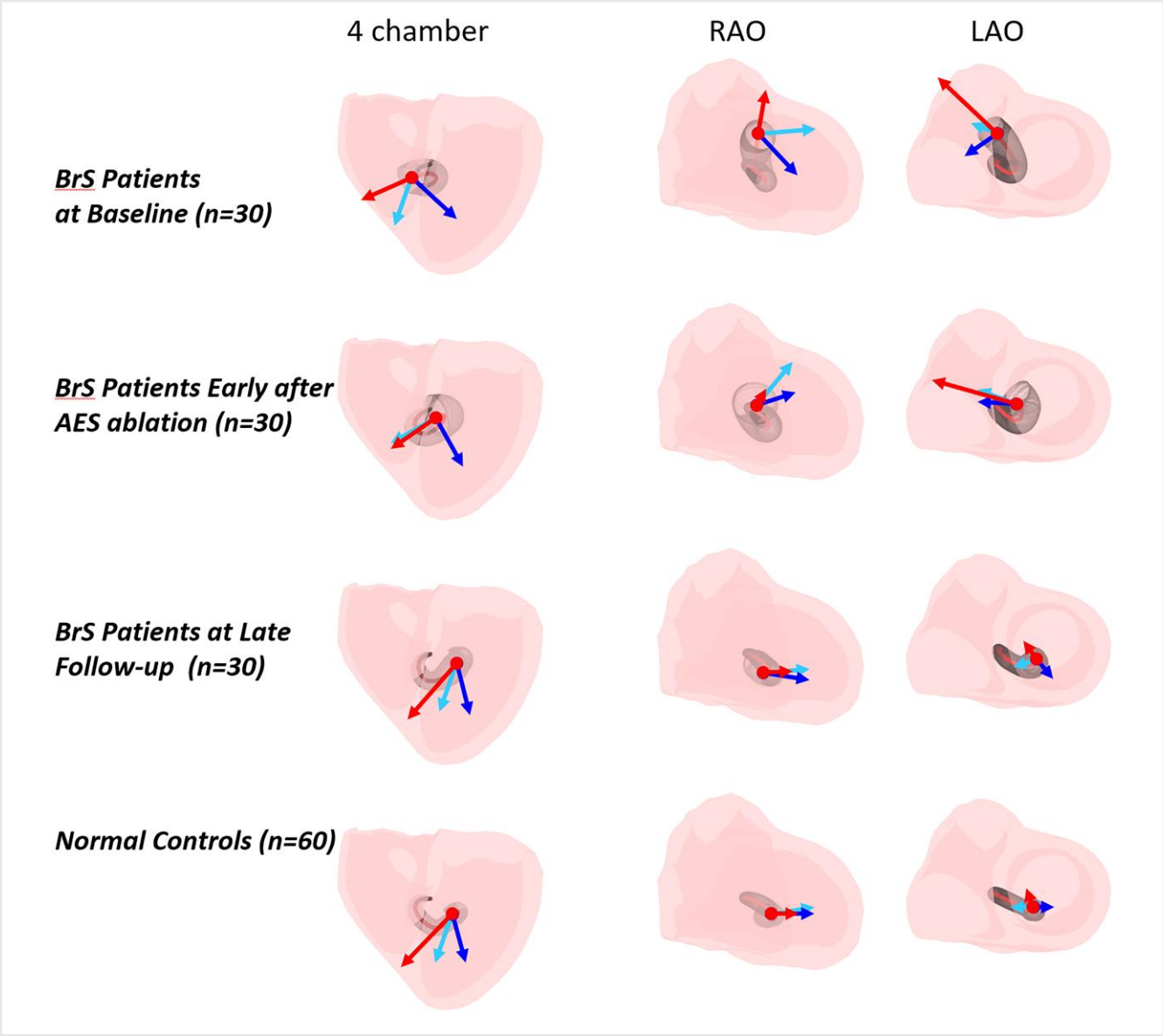

Figure 3 Average terminal QRS, ST-Tpeak, and Tpeak-Tend direction for Brugada patients and normal controls. The ventricles are projected in standard cardiac views as follows: four chambers (left panels), right anterior oblique view (RAO, middle panels), and left anterior oblique (LAO, right panels). The red arrow shows terminal-QRS-CineECG direction (110–150 ms after QRS onset), the light blue arrow the ST-Tpeak, and the blue arrow the TpTe. In Brugada syndrome (BrS) patients, at baseline, the Terminal-QRS points towards right ventricular outflow tract (RVOT) (upper panels), early after arrhythmogenic substrate (AS) radiofrequency ablation it moves leftward (upper middle panels) and shifting clearly leftward at late follow-up (lower middle panels). In normal controls, the mean Terminal-QRS direction always points leftward (lower panels). RAO, right anterior oblique; LAO, left anterior oblique; BrS, Brugada syndrome; RVOT, right ventricular outflow tract; AS, arrhythmogenic substrate.

apex–base axes) (*Table 4*, *Figures 2–5*, Supplementary material online, *Web-Movie S4*).

Most CineECG parameters at late FU were significantly different, when compared to baseline and to early after EPI-AS-RFA, while very few significant differences in CineECG location and direction were observed between BrS patients at late FU and normal controls (*Tables 3* and *4*). While in BrS patients at baseline and early after EPI-AS-RFA, most CineECG activity was prevalently localized in RV/RVOT, at late FU, as in normal age- and sex-matched controls, CineECG activity was prevalent in LV and never localized in RV/RVOT, either during depolarization (QRS and Terminal-QRS) or during repolarization (ST-Tend, ST-Tpeak, and Tpeak-Tend; *Tables 3* and *4*, *Figures 2* and *3*, Supplementary material online, *Web-Movie S1*). As to the CineECG classification, at late FU, 87% of BrS patients were classified 'Normal', and 13% as 'Undetermined', while none were any longer classified as 'Brugada' or 'RBBB' (*Table 5*).

Discussion

In this study, CineECG, in parallel with 12-lead ECG, showed a complex temporo-spatial perturbation of *both* depolarization and repolarization in BrS patients, prevalently localized in RV/RVOT, which progressively

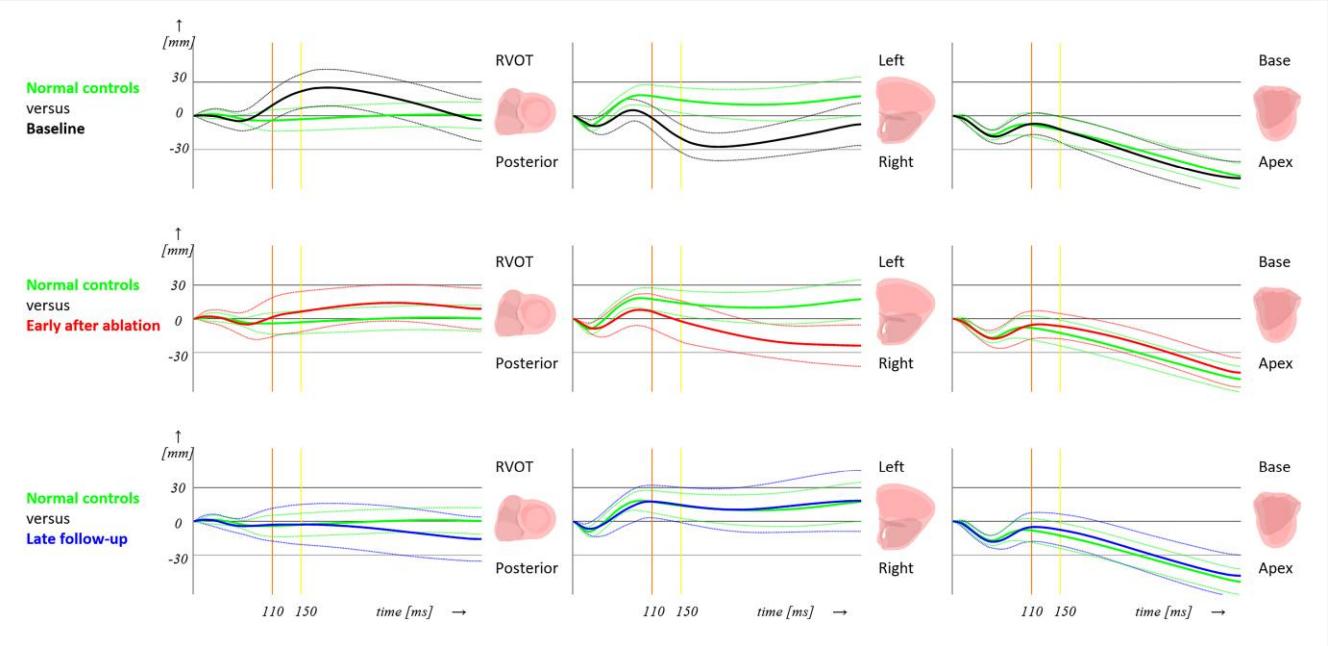

Figure 4 Average Terminal-QRS, ST-Tpeak, and Tpeak-Tend *m*TSI location for Brugada patients per *x*–*y*–*z* heart axes. The three orthogonal *x*–*y*–*z* heart axes are used to plot the location of *m*TSI within the heart (*x*-axis in left panels, *y*-axis middle panels, *z*-axis in right panels). On the abscissa is the time (yellow vertical line correspond to 110 ms, red line to 150 ms), and on the ordinate, the displacement relative to the starting point of the *m*TSI (left septum). Solid green lines are the average *m*TSI path per heart axis, and the dotted lines the standard deviation derived from the normal controls. These normal values serve as a reference vs. Brugada patients at baseline (black lines in top panels), early after ablation (red lines middle panels), and at late follow-up (blue lines in the bottom panels). Clearly visible is the deviating location of the Terminal-QRS and ST-Tpeak towards right ventricular outflow tract (RVOT) in *x*-axis and towards right ventricle (RV) (*y*-axis) at baseline. RVOT, right ventricular outflow tract; RV, right ventricle.

normalized after epicardial ablation. Of note, CineECG, enabling a direct 3D temporo-spatial correlation between electrical forces to their anatomical cardiac sources,[6,7,14] allowed a more precise temporo-spatial localization of the cardiac electrical activity, which could not have been clearly esteemed from the standard 12-lead ECGs.

Specifically, CineECG revealed that in spontaneous type-1 BrS patients at baseline, both depolarization and repolarization electrical activity had a prevalent location in RV/RVOT, concordant with the AS area detected by epicardial mapping. While we had already described the abnormal RVOT localization detect by CineECG during late depolarization in BrS patients,[21] in this study, CineECG newly detected an abnormal and unexpected RVOT localization also during repolarization (ST-Tpeak and Tpeak-Tend intervals). Such abnormal RV/RVOT location, both during repolarization and repolarization, was never present in normal age- and sex-matched subjects and was progressively normalized after epicardial substrate ablation.

Twelve-lead electrocardiogram characteristics of depolarization and repolarization in Brugada syndrome patients at baseline

In this study, we observed that QRS duration measured on the RMS of the 12-lead ECG was longer in BrS patients than in normal controls. Unexpectedly, the maximum QRS amplitude of the RMS of the 12-lead ECG was significantly lower in BrS patients at baseline than in normal controls, while the amplitude of the terminal QRS (at 110–150 ms) was significantly higher, possibly suggesting desynchronization and fragmentation of depolarization in BrS patients at baseline, compared to normal controls (see *Table 2*). As to repolarization, QTc duration was longer, while maximum T-wave amplitude was lower in BrS patients than in normal controls, indicating a perturbation of *both* depolarization and repolarization in BrS patients.

CineECG characteristics of depolarization and repolarization in Brugada syndrome patients at baseline

In this subset of high-risk BrS patients with spontaneous type-1 pattern before and after EPI-AS-RFA, none of them being included in our previous studies, the non-invasive CineECG detected an abnormal RVOT location of late depolarization forces, coincident with the AS localization detected by epicardial PDMs. Such abnormal RVOT location was previously observed both in patients with spontaneous type-1 BrS pattern, and in patients developing type-1 BrS pattern during ajmaline test,[21,22] even before ajmaline infusion. Vice versa, a late RVOT depolarization was never observed in normal subjects, or in RBBB, or in ajmaline-negative patients.[21,22]

Unexpectedly, CineECG detected a prevalence of electrical forces in RVOT also during early repolarization (both during ST-Tpeak and Tpeak-Tend intervals). These new findings may indicate that BrS affects both depolarization and repolarization, rather supporting the hypothesis of a combined delay of depolarization and repolarization affecting the RV/RVOT area.[6,9,17,18] Notoriously, repolarization is more complex than depolarization, being a slower and much more heterogeneous process, with intramural and regional differences, comprising

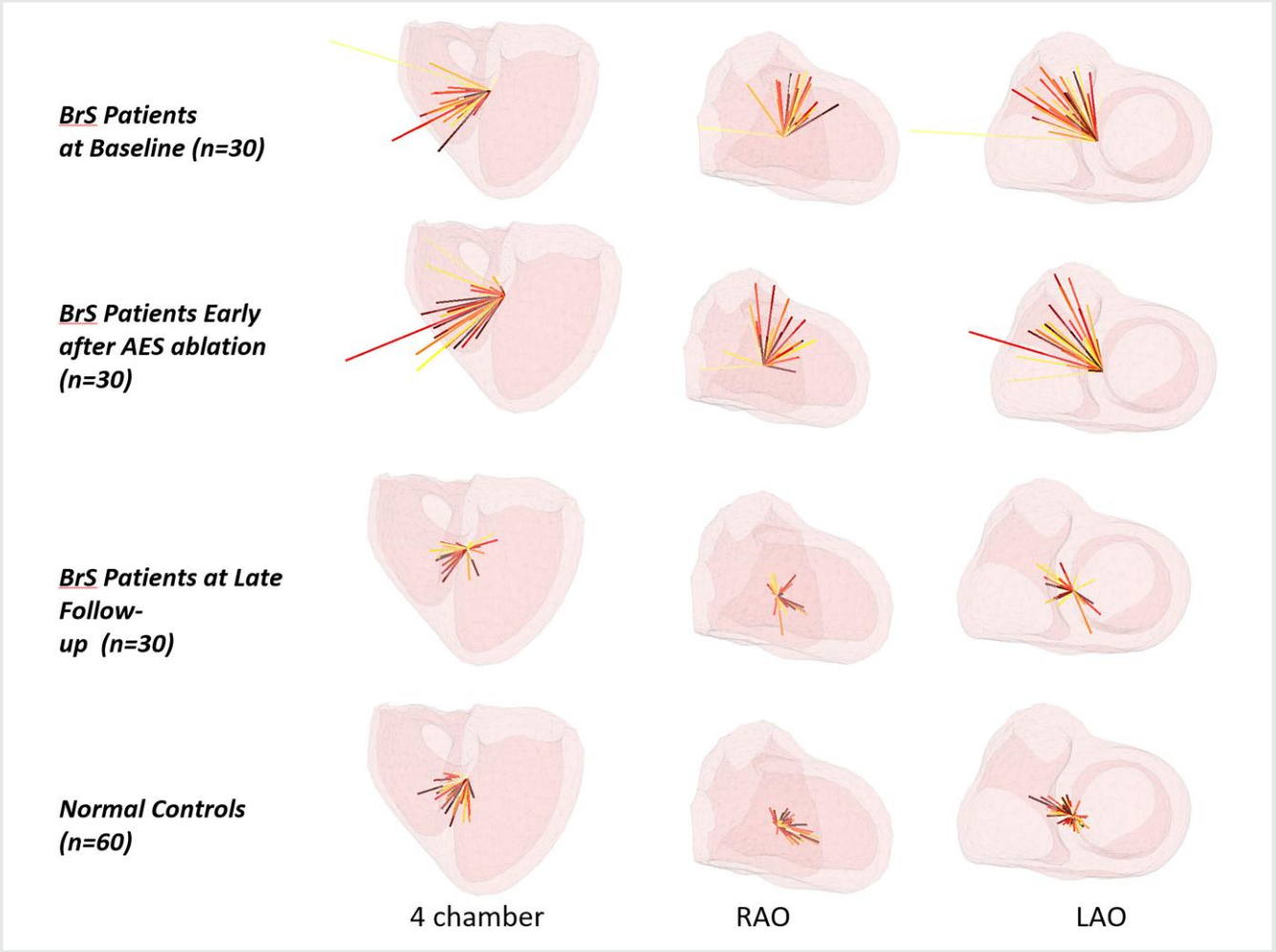

Figure 5 Individual Terminal-QRS amplitude-directions for Brugada patients and normal controls. The last part of the QRS direction is shown by a line, where the length of the line represents average amplitude of the terminal QRS. The ventricles are projected in standard cardiac views as follows: four chambers (left panels), right anterior oblique (RAO, middle panels), and left anterior oblique (LAO, right panels). For each subject, the terminal QRS amplitude—direction is plotted by a different colour. In BrS patients, at baseline, Terminal-QRS directions are mainly oriented towards right ventricular outflow tract (RVOT)/right ventricle (RV) with significant amplitude values (upper panels). Early after arrhythmogenic substrate radiofrequency ablation (EPI-AS-RFA, in upper middle panels), the Terminal-QRS points less towards the RVOT. At late follow-up, the QRS terminal shifts clearly leftward with lower amplitude values in the normal range (lower middle panels). In normal controls, Terminal-QRS points frequently leftward with limited average amplitude values (lower panels). RAO, right anterior oblique; LAO, left anterior oblique; RVOT, right ventricular outflow tract; RV, right ventricle; EPI-AS-RFA, early after arrhythmogenic substrate radiofrequency ablation.

the fact that in certain regions, repolarization may start when depolarization is still ongoing in other regions. CineECG cannot attribute a given shift either to depolarization or repolarization, since it encompasses the localization of the summation of all depolarization and repolarizations forces at any given time, depicting this combined temporo-spatial localization as a continuous trajectory. However, the abnormal RV/RVOT localization of electrical forces in BrS patients at baseline occurred beyond the terminal QRS, during the ST-Tpeak interval, which is generally defined as repolarization in standard ECG. Of note, the CineECG alterations homogeneously observed in BrS patients were quite specific, and different from the CineECG modifications recently observed in Familial ST-Segment Depression Syndrome patients, who showed an increased electrical activation pathway towards the base of the heart during the entire repolarization phase.[29] Hence, the interpretation of the repolarization abnormalities in BrS patients still requires further investigation.

Ventricular repolarization abnormalities in Brugada syndrome patients

Hitherto, few studies focused on repolarization in BrS patients. Early experimental studies showed that the instability and heterogeneity of repolarization at epicardial RVOT were associated with arrhythmogenesis in patients and *in vitro* tissue models of BrS.[6,7,12,14] While previous scattered reports suggested that terminal T-wave components (ST-Tpeak and Tpeak-Tend) might be predictors of ventricular arrhythmic events in BrS patients, in a larger study, Tpeak-Tend was not significantly prolonged in type-1 BrS patients, similar to normal subjects.[24] In this study, the corrected QT duration was slightly but homogeneously longer in BrS patients at baseline, compared to late follow-up after EPI-AS-RFA and to normal controls. This may mainly depend on longer QRS duration, although also ST-Tpeak and Tpeak-Tend durations were slightly

Table 5 CineECG classification based on predefined CineECG classes

Group	CineECG classification (%, n)			
	Normal	RBBB	Brugada	Undetermined
BrS patients at baseline ($n = 30$)	0	0	100% *(30)*	0
BrS patients early after AS-RFA ($n = 30$)	67% *(20)*	3% *(1)*	10% *(3)*	20% *(6)*
BrS patients at late follow-up ($n = 30$)	87% *(26)*	0	0	13% *(4)*
Normal controls ($n = 60$)	100% *(30)*	0	0	0

According to the predefined CineECG classes, all BrS patients at baseline were correctly classified as 'Brugada', and all Normal controls were correctly classified as 'Normals'. Early after the AS-RFA, one patient was classified as 'RBBB', and three patients remained still classified as 'Brugada', while the vast majority (87%) became 'Normal' or 'Undetermined'. At late follow-up, most BrS patients (87%) were classified as 'Normals', and a minority as 'Undetermined' (13%), while none as 'Brugada' or 'RBBB'. Significance of italic values represents number of patients.
AS-RFA, arrhythmogenic substrate radiofrequency ablation.

longer at baseline, compared to late follow-up and to normal controls (*Table 2*).

Correlation of 12-lead electrocardiogram and CineECG to the arrhythmogenic substrate area

We consistently observed the concordance of the abnormal RV/RVOT localization detected by CineECG, with the spontaneous type-1 pattern on upper precordial lead on 12-lead ECG, and with the arrhythmogenic surface area detected by epicardial electro-anatomical mapping. Besides, both RVOT location, and type-1 pattern, disappeared after the complete arrhythmogenic surface ablation, normalizing almost all 12-lead ECG and CineECG depolarization and repolarization parameters. The possibility to detect the arrhythmogenic substrate area, and to determine its size, by non-invasive methods, would be valuable for the risk stratification of BrS patients, particularly since previous studies showed that the size of the arrhythmogenic substrate area is associated with the severity of the disease.[11,12] However, in this sample, we could not find any specific correlation with any 12-lead ECG or CineECG parameters and the size of the arrhythmogenic substrate area.

Twelve-lead electrocardiogram and CineECG changes after arrhythmogenic substrate ablation

CineECG, in parallel with 12-lead ECG, showed a progressive normalization of both depolarization and repolarization wavefront after epicardial RVOT arrhythmic substrate ablation. In 12-lead ECG, after EPI-AS-RFA, QRS duration and QTc shortened, while maximal QRS amplitude increased, while terminal-QRS amplitude decreased. In CineECG, while EPI-AS-RFA immediately abolished the RVOT location of the late depolarization forcers (Terminal-QRS), together with type-1 BrS pattern, the CineECG wavefront during ST-Tpeak and Tpeak-Tend took longer to normalize. At late follow-up after EPI-AS-RFA, both depolarization and repolarization normalized, with CineECG wavefront becoming prevalent in LV, like in normal controls. Moreover, QRS amplitude significantly increased in the late follow-up after ablation, although in parallel with QRS shortening, indicating the normalization of the depolarization process after the ablation of the arrhythmogenic substrate, although limited differences in the 12-lead ECG still subsist among BrS patients and normal controls. At CineECG, early after EPI-AS-RFA, the RV/RVOT location of late depolarization forces immediately disappeared in most BrS patients, in parallel with type-1 BrS pattern elimination. Of note, the repolarization wavefront took longer to normalize, with residual CineECG forces still lingering in the RV anterior wall, mirrored by unspecific ST-Tpeak abnormalities in 12-lead ECG (*Figure 2*, and Supplementary material online, *Appendix-B* Individual Patients' Material).

The temporal discrepancy between depolarization and repolarization changes after ablation may be due to the cardiac memory phenomenon being more typical of ventricular repolarization.[30,31] Alternatively, it may be caused by acute effects of radiofrequency ablation,[10,11] generally disappearing within 1–2 h after the procedure. This effect may be related to specific properties of the Brugada cells reacting to thermal changes during the RF ablation, not observed in non-Brugada patients undergoing epicardial ablation.[32] Alternatively, the temporary persistence of abnormal repolarization in RVOT area early after EPI-AS-RFA may be due to cardiac memory, impairing ventricular repolarization normalization after arrhythmias or pacing.[30,31]

The abnormal late depolarization forces in RV/RVOT at CineECG disappeared at late follow-up, when the CineECG almost completely normalized, with both repolarization and depolarization wavefront mainly localized in septum and LV, becoming like the age- and sex-matched normal controls (*Tables 2–4*, *Figures 3–5*, Supplementary material online, *Web-Movies S1–S3*).

Clinical implications of CineECG findings in management of Brugada syndrome patients

The interpretation of the 12-lead ECG tracings in patients with suspected BrS is very challenging, even for expert cardiologists.[26,33] This study does not intend to underplay the validity of previously developed 12-lead ECG parameters for the characterization of BrS patients. Rather, the scope of this study was to integrate previously validated 12-lead ECG parameters by novel CineECG parameters, thus improving visualization of the electrical abnormalities detected in BrS patients before and after EPI-AS-RFA.

The RVOT localization of depolarization and repolarization correlates not only with the type-1 BrS pattern but also with the AS identification by epi-PDM in BrS patients. Hence, the abolition of RVOT localization, concomitant with the normalization of the type-1 pattern, may indicate that AS is no longer present after EPI-AS-RFA. In this regard, CineECG can integrate the 12-lead ECG, providing a new non-invasive mapping system, opening new perspectives for the diagnostic and prognostic evaluation of BrS patients.

The multiparametric CineECG classification 'Brugada' may disclose the presence of an arrhythmogenic substrate in RVOT, indicating

potential high-risk BrS patients. Conversely, the CineECG classification 'Normal' may hint that a sizeable AS is not present. Thus, CineECG may contribute to the risk stratification of BrS patients, guiding the use of diagnostic provocative ajmaline tests. However, this hypothesis still needs to be validated in specifically designed studies.

Based on CineECG diagnostic classes, while all BrS patients at baseline were classified as 'Brugada', after AS ablation, most patients (87%) became classified 'Normal'. The normalization of CineECG parameters after AS ablation in BrS patients during late follow-up may support the efficacy and safety of low-energy epicardial EPI-AS-RFA, removing the fragmented and delayed AS, without producing scars or transmural lesions,[10,11] but also this observation requires further validation in a specifically designed study.

Limitations

Additional larger prospective studies are needed to confirm the diagnostic and prognostic role of CineECG in routine clinical practice. Also, further studies need to verify the ability of CineECG to discriminate BrS phenocopies and near-normal conditions,[26,33] such as incomplete RBBB, likely to be labelled as 'Undetermined'.

The use of a standard 3D-heart model for CineECG was felt appropriate, since all BrS patients and normal controls had normal cardiac and BMI dimensions.[22,23] In future applications, a personalized 3D-heart/torso model, considering individual biometrical information, will provide an optimized projection of electrical forces fitting the individual cardiac structure.

CineECG used a generic torso/heart model, ignoring the exact location of the RV and RVOT relative to the electrodes. While the electrode positions can have a significant effect on 12-lead ECG waveforms, the effect on CineECG was shown to be small for limited spatial changes, such as the modified precordial leads utilized for BrS diagnosis.[22,23] Further studies need to investigate the modifications in CineECG pathway when using a patient specific vs. a generic heart–torso model, and normal vs. modified precordial lead positions. Of note, we observed full normalization after EPI-AS-ATC in BrS patients, without significant differences with normal controls, despite the fact that in some BrS patients, modified precordial leads were used, rather than normal leads. In this regard, the modified lead position, maximizing the chance to find any BrS pattern, should have generated larger differences (and certainly not lesser differences) between BrS patients and normal controls, where normal precordial lead configuration was always utilized. In any case, the effect of modified vs. normal leads on CineECG needs to be further explored, also in personalized torso models.

CineECG, encompassing the summation of depolarization and repolarizations forces at any given time, and depicting this combined temporo-spatial localization as a continuous trajectory, does not have the possibility to attribute any given shift either to depolarization or repolarization. The localization of repolarization is less straightforward than the localization of depolarization, since the repolarization process is less uniform over the heart and last longer. CineECG cannot discriminate whether changes occurring during early ST were attributed to depolarization or repolarization abnormalities, however, for abnormalities occurring during the ST-segment, the contribution of depolarization forces is likely to be progressively diminishing, while repolarization forces increase.

The precise correlation between CineECG wavefront and any given cardiac structure, and specifically to RVOT region is still approximate. We observed that CineECG before ablation pointed towards the RVOT region in the generic heart/torso model. A more precise patient-specific localization of the arrhythmogenic substrate to the heart anatomy (RVOT and/or RV anterior wall) will be possible when introducing an individual patient-specific model.

In specific conditions affecting repolarization and modifying the ST-segment, such as delayed activation in Familial ST depression, CineECG could localize abnormalities to specific regions of the heart, as shown by Frosted *et al.*[29] Preliminary studies during acute ischaemia show similar results.

In this study, the AS area extent, known to be associated with BrS severity and VT/VF vulnerability,[10,11,14] could not be correlated to a single or multiple 12-lead ECG or CineECG parameters. This may be due to the limited sample size, including all high-risk patients with relatively large AS areas during ajmaline infusion. It may be necessary to such correlation in a cohort of BrS patients with a wider array of arrhythmogenic area size, to be able to detect any significant correlation.

Moreover, further studies are required to better define the best CineECG parameters to describe and quantify ventricular repolarization, considering sex and gender, known to be important determinant of ventricular repolarization variability.[27,34]

In this subset of high-risk BrS patients with spontaneous type-1 pattern, CineECG patterns were quite homogeneous, regardless of genotypic background. However, the still limited number of patients with known genotype impairs the possibility to draw definitive correlations between CineECG findings and different genotype.

Conclusions

CineECG, in parallel with 12-lead ECG, showed a complex temporo-spatial perturbation of *both* depolarization and repolarization in BrS patients, which normalized after epicardial ablation. Of note, CineECG allowed a more precise temporo-spatial localization of the cardiac electrical activity during the terminal depolarization and early repolarization phase to the RV/RVOT region, which could not be clearly esteemed from the standard 12-lead ECGs. Such localization was congruent with the substrate area detected by epi-PDMs. CineECG normalization, in parallel with the disappearance of the type-1 BrS pattern, may mirror the elimination of AS through the epicardial ablation procedure. CineECG can integrate the 12-lead ECG, providing a new non-invasive mapping system, capable of uncovering the presence of the AS in a BrS patient. This opens new perspectives for the diagnostic and prognostic evaluation of BrS patients. In the future, such approach may contribute to better electrocardiographic characterization of other arrhythmogenic-cardiomyopathies.

Authors' contributions

E.T.L., P.M.V.D., G.C., and M.B.: conceptualization, formal analysis, data curation, writing—original draft, and visualization. F.H.: statistical analysis and writing. G.V., E.M., Z.C., L.A., and V.S.: writing—review and editing and validation. C.P.: conceptualization, methodology, validation, writing—review and editing, and supervision. All authors contributed to the article and approved the submitted version.

Supplementary material

Supplementary material is available at *European Heart Journal – Digital Health*.

Funding

This study was partially supported by 'Ricerca Corrente' funding from the Italian Ministry of Health to IRCCS Policlinico San Donato, Milan, Italy.

Conflict of interest: P.M.V.D. is an owner of Peacs-BV and ECG Excellence BV, currently in the process of commercialization of the CineECG algorithms. The other authors declare that the research

was conducted in the absence of any commercial or financial relationships that could be construed as a potential conflict of interest.

Data availability

The original contributions presented in the study are included in the article/supplementary material; further inquiries can be directed to the corresponding author.

References

1. Antzelevitch C, Brugada P, Borggrefe M, Brugada J, Brugada R, Corrado D, *et al.* Brugada syndrome: report of the second consensus conference: endorsed by the Heart Rhythm Society and the European Heart Rhythm Association. *Circulation* 2005;**111**:659–670.
2. Pappone C, Santinelli V. Brugada syndrome: progress in diagnosis and management. *Arrhythm Electrophysiol Rev* 2019;**8**:13–18.
3. Priori SG, Blomstrom-Lundqvist C, Mazzanti A, Blom N, Borggrefe M, Camm J, *et al.* 2015 ESC Guidelines for the management of patients with ventricular arrhythmias and the prevention of sudden cardiac death: the task force for the management of patients with ventricular arrhythmias and the prevention of sudden cardiac death of the European Society of Cardiology (ESC) endorsed by: Association for European Paediatric and Congenital Cardiology (AEPC). *Europace* 2015;**17**:1601–1687.
4. Ciconte G, Monasky MM, Santinelli V, Micaglio E, Vicedomini G, Anastasia L, *et al.* Brugada syndrome genetics is associated with phenotype severity. *Eur Heart J* 2021;**42**:1082–1090.
5. Postema PG, Walsh R, Bezzina CR. Illuminating the path from genetics to clinical outcome in Brugada syndrome. *Eur Heart J* 2021;**42**:1091–1093.
6. Postema PG, van Dessel PFHM, Kors JA, Linnenbank AC, van Herpen G, van Eck HJR, *et al.* Local depolarization abnormalities are the dominant pathophysiologic mechanism for type 1 electrocardiogram in Brugada syndrome a study of electrocardiograms, vectorcardiograms, and body surface potential maps during ajmaline provocation. *J Am Coll Cardiol* 2010;**55**:789–797.
7. Zhang JJ, Sacher F, Hoffmayer K, O'Hara T, Strom M, Cuculich P, *et al.* Cardiac electrophysiological substrate underlying the ECG phenotype and electrogram abnormalities in Brugada syndrome patients. *Circulation* 2015;**131**:1950.
8. Morita H, Fukushima-Kusano K, Nagase S, Takenaka-Morita S, Nishii N, Kakishita M, *et al.* Site-specific arrhythmogenesis in patients with Brugada syndrome. *J Cardiovasc Electrophysiol* 2003;**14**:373–379.
9. Morita H, Zipes DP, Fukushima-Kusano K, Nagase S, Nakamura K, Morita ST, *et al.* Repolarization heterogeneity in the right ventricular outflow tract: correlation with ventricular arrhythmias in Brugada patients and in an in vitro canine Brugada model. *Heart Rhythm* 2008;**5**:725–733.
10. Brugada J, Pappone C, Berruezo A, Vicedomini G, Manguso F, Ciconte G, *et al.* Brugada syndrome phenotype elimination by epicardial substrate ablation. *Circ-Arrhythmia Elec* 2015;**8**:1373–1381.
11. Pappone C, Brugada J, Vicedomini G, Ciconte G, Manguso F, Saviano M, *et al.* Electrical substrate elimination in 135 consecutive patients with Brugada syndrome. *Circ-Arrhythmia Elec* 2017;**10**:e005053.
12. Pappone C, Ciconte G, Manguso F, Vicedomini G, Mecarocci V, Conti M, *et al.* Assessing the malignant ventricular arrhythmic substrate in patients with Brugada syndrome. *J Am Coll Cardiol* 2018;**71**:1631–1646.
13. Chokesuwattanaskul R, Nademanee K. Advances in ventricular arrhythmia ablation for Brugada syndrome. *Card Electrophysiol Clin* 2022;**14**:685–692.
14. Ciconte G, Santinelli V, Vicedomini G, Borrelli V, Monasky MM, Micaglio E, *et al.* Non-invasive assessment of the arrhythmogenic substrate in Brugada syndrome using signal-averaged electrocardiogram: clinical implications from a prospective clinical trial. *Europace* 2019;**21**:1900–1910.
15. Pappone C, Mecarocci V, Manguso F, Ciconte G, Vicedomini G, Sturla F, *et al.* New electromechanical substrate abnormalities in high-risk patients with Brugada syndrome. *Heart Rhythm* 2020;**17**:637–645.
16. Pappone C, Santinelli V, Mecarocci V, Tondi L, Ciconte G, Manguso F, *et al.* Brugada syndrome: new insights from cardiac magnetic resonance and electroanatomical imaging. *Circ-Arrhythmia Elec* 2021;**14**:1024–1036.
17. Antzelevitch C, Patocskai B. Brugada syndrome: clinical, genetic, molecular, cellular, and ionic aspects. *Curr Prob Cardiology* 2016;**41**:7–57.
18. Wilde AAM, Postema PG, Di Diego JM, Viskin S, Morita H, Fish JM, *et al.* The pathophysiological mechanism underlying Brugada syndrome depolarization versus repolarization. *J Mol Cell Cardiol* 2010;**49**:543–553.
19. van Dam PM. A new anatomical view on the vector cardiogram: the mean temporal–spatial isochrones. *J Electrocardiol* 2017;**50**:732–738.
20. van Dam PM, Boonstra M, Locati ET, Loh P. The relation of 12 lead ECG to the cardiac anatomy: the normal CineECG. *J Electrocardiol* 2021;**69**:67–74.
21. van Dam PM, Locati ET, Ciconte G, Borrelli V, Heilbron F, Santinelli V, *et al.* Novel CineECG derived from standard 12-lead ECG enables right ventricle outflow tract localization of electrical substrate in patients with Brugada syndrome. *Circ-Arrhythmia Elec* 2020;**13**:e008524.
22. Boonstra MJ, Brooks DH, Loh P, van Dam PM. CineECG: a novel method to image the average activation sequence in the heart from the 12-lead ECG. *Comput Biol Med* 2022;**141**:105128.
23. Boonstra MJ, Hilderink BN, Locati ET, Asselbergs FW, Loh P, van Dam PM. Novel CineECG enables anatomical 3D localization and classification of bundle branch blocks. *Europace* 2021;**23**:i80–i87.
24. Mugnai G, Hunuk B, Hernandez-Ojeda J, Stroker E, Velagic V, Ciconte G, *et al.* Role of electrocardiographic Tpeak-Tend for the prediction of ventricular arrhythmic events in the Brugada syndrome. *Am J Cardiol* 2017;**120**:1332–1337.
25. Wagner P, Strodthoff N, Bousseljot RD, Kreiseler D, Lunze FI, Samek W, *et al.* PTB-XL, a large publicly available electrocardiography dataset. *Sci Data* 2020;**7**:154.
26. Chevallier S, Forclaz A, Tenkorang J, Ahmad Y, Faouzi M, Graf D, *et al.* New electrocardiographic criteria for discriminating between Brugada types 2 and 3 patterns and incomplete right bundle branch block. *J Am Coll Cardiol* 2011;**58**:2290–2298.
27. Merri M, Benhorin J, Alberti M, Locati E, Moss AJ. Electrocardiographic quantitation of ventricular repolarization. *Circulation* 1989;**80**:1301–1308.
28. Kawada S, Morita H, Antzelevitch C, Morimoto Y, Nakagawa K, Watanabe A, *et al.* Shanghai score system for diagnosis of Brugada syndrome: validation of the score system and system and reclassification of the patients. *JACC Clin Electrophysiol* 2018;**4**:724–730.
29. Frosted R, Paludan-Muller C, Vad OB, Olesen MS, Bundgaard H, van Dam P, *et al.* CineECG analysis provides new insights into familial ST-segment depression syndrome. *Europace* 2023;**25**:euad116.
30. Coronel R, Opthof T, Plotnikov AN, Wilms-Schopman FJG, Shlapakova IN, Danilo P, *et al.* Long-term cardiac memory in canine heart is associated with the evolution of a transmural repolarization gradient. *Cardiovasc Res* 2007;**74**:416–425.
31. Janse MJ, Sosunov EA, Coronel R, Opthof T, Anyukhovsky EP, de Bakker JMT, *et al.* Repolarization gradients in the canine left ventricle before and after induction of short-term cardiac memory. *Circulation* 2005;**112**:1711–1718.
32. Pappone C, Ciconte G, Anastasia L, Gaita F, Grant E, Micaglio E, *et al.* Right ventricular epicardial arrhythmogenic substrate in long-QT syndrome patients at risk of sudden death. *Europace* 2023;**25**:948–955.
33. Gottschalk BH, Anselm DD, Brugada J, Brugada P, Wilde AA, Chiale PA, *et al.* Expert cardiologists cannot distinguish between Brugada phenocopy and Brugada syndrome electrocardiogram patterns. *Europace* 2016;**18**:1095–1100.
34. Locati ET, Bagliani G, Padeletti L. Normal ventricular repolarization and QT interval: ionic background, modifiers, and measurements. *Card Electrophysiol Clin* 2017;**9**:487–513.